This journal is (c) The Royal Society of Chemistry 2010

Supporting Information for:

Hydrogen Storage and Carbon Dioxide Capture in an Iron-Based Sodalite-Type Metal-Organic Framework (Fe-BTT) Discovered via High-Throughput Methods

Kenji Sumida, Satoshi Horike, Steven S. Kaye, Zoey R. Herm, Wendy L. Queen, Craig M. Brown, Fernande Grandjean, Gary J. Long, Anne Dailly, Jeffrey R. Long*

Department of Chemistry, University of California, Berkeley, CA 94720-1460

Center for Neutron Research, National Institute of Standards and Technology, Gaithersburg, MD 20899

Department of Materials Science and Engineering, University of Maryland, College Park, MD 20742

Department of Physics, B5, University of Liège, B-4000 Sart-Tilman, Belgium

Department of Chemistry, Missouri University of Science and Technology, University of Missouri, Rolla, Missouri 65409

Chemical and Environmental Sciences Laboratory, General Motors Company, Warren, Michigan 48090

email: jrlong@berkeley.edu

Chem. Sci.

Experimental Details

Unless otherwise stated, all manipulations were performed under an inert dinitrogen or helium atmosphere. 1,3,5-Tris(2*H*-tetrazol-5-yl)benzene hydrochloride (H_3BTT·2HCl) was prepared according to the literature procedure.[1] All other reagents were obtained from commercial vendors and used without further purification. ***Caution***. Tetrazolate compounds are potentially explosive, and should be handled with care. While we did not encounter any difficulties in handling the free ligand H_3BTT·2HCl or the frameworks derived therein, care should be taken to avoid generating sparks or creating friction on the material. In particular, a teflon-lined spatula should be used when handling the desolvated form of Fe-BTT.

$Fe_3[(Fe_4Cl)_3(btt)_8]_2$·22DMF·32DMSO·$11H_2O$ (solvated FeBTT). Anhydrous ferrous chloride (76 mg, 0.59 mmol), H_3BTT·2HCl (58 mg, 0.20 mmol), DMF (5 mL), and DMSO (5 mL) were added to a 20 mL scintillation vial, and the vial was tightly sealed with a teflon-lined cap. The reaction mixture was heated on a hotplate at 110 °C for 24 h, after which time small, pale yellow crystals were formed on the vial walls. The solid was filtered and washed with DMF, and isolated as a pale yellow-green solid (42 mg, 32%). IR (neat): 3391 (m br), 3002 (w), 2920 (w), 1654 (s), 1498 (w), 1435 (m), 1412 (s), 1389 (m), 1314 (w), 1253 (w), 1227 (w), 1194 (w), 1102 (w), 1014 (s), 951 (s), 904 (m), 788 (s), 749 (m), 661 (w). Anal. Calcd for $C_{274}H_{416}Cl_6Fe_{27}N_{214}O_{65}S_{32}$: C, 31.36; H, 4.00; N, 28.56. Found: C, 31.19; H, 4.05; N, 28.32. The solvent composition was deduced using a combination of elemental analysis data and thermogravimetric analysis. The DMF-solvated framework was generated by suspending **1** within DMF at 80 °C for 24 h, with exchanging of the solvent for fresh DMF each 8 h. IR (neat): 3178 (br s), 2927 (m), 2857 (m), 1656 (s) 1498 (m), 1437 (m), 1408 (s), 1385 (s), 1254 (m), 1090 (s), 1062 (m), 951 (w), 907 (w), 865 (w), 788 (m), 749 (w), 696 (w), 678 (w), 658 (s). The methanol-solvated framework was generated by suspending the DMF-solvated material in MeOH at 100 °C for 48 h, exchanging the solvent for fresh MeOH each 8 h. IR (neat): 3178 (br s), 2943 (m), 2831 (m), 1416 (s), 1231 (w), 1194 (w), 1133 (w), 1069 (w), 1012 (s), 902 (w), 789 (s), 750 (m), 688 (w), 645 (w). The sample is air- and moisture-sensitive, and was stored in a solvent-free glove box under dinitrogen.

High-Throughput Experiments. High-throughput experiments were performed using a robotic Symyx Core Module System equipped with powder- and liquid-dispensing functionality. The main features of the robot deck are shown in Figure S1. The recipes for the screening reactions were programmed from a client computer terminal using Symyx Library Studio version 7.1.7.14, and the automated dispensing protocols were executed through Symyx Automation Studio version 1.1.1.8. These client-side software applications communicate to the Core Module through a central server, which maintains a database containing all experimental parameters. The Core Module is loaded within a Braun glovebox under a dinitrogen atmosphere, and the pneumatic valves were operated using a dinitrogen supply with a pressure maintained at 80 psi.

Powder dispensing was performed by loading finely-ground metal salts and ligands into plastic powder-dispensing hoppers. The solid was dispensed by automatic transfer of the individual vials onto a Sartorius LP 1200.S balance on the Core Module deck with a measurement error of less than 0.1 mg. Stability of the balance was achieved through sealing of the balance headspace using a polymer membrane with a circular opening that allows for lowering of the powder hopper to a position just above the aperture of the vial. Following taring of the weight of the empty vial, the appropriate quantity of solid was dispensed by the robot arm. The discrepancy between the mass dispensed and the programmed mass was typically within 2%.

Liquid dispensing was achieved by firstly placing vials filled with neat solvents on the robot deck in positions as input in the Automation Studio protocol. The vials were sealed with scepta to avoid cross-contamination or evaporation of the solvents. The liquids were aspirated through a needle that is located on the right arm, and is connected to a series of three syringe pumps with volumes of 0.5 mL, 3 mL, and 5 mL, respectively. The syringe used depended upon the quantity of the liquid to be dispensed. Once the liquid is aspirated, the needle is moved to the appropriate vials through movements of the right arm. The protocol was such that the needle was thoroughly washed with methylene chloride following each solvent, to avoid cross-contamination.

Automated dispensing of the products onto glass plates for powder X-ray analysis was achieved by a protocol that firstly aspirates the mother liquid from the reaction product, and replenishes it the vial with fresh DMF. This procedure was repeated three times, followed by a similar washing procedure using methylene chloride. The crystals were then pulverized using the automated shaker system on the robot deck with small ball bearings, and the resulting slurry was

dispensed into individual wells of a crystallizer block attached to a glass plate. The methylene chloride was then allowed to evaporate, and the crystallizer block was removed from the glass plate. The plate was then mounted onto a metal frame, and subsequently transferred to the high-throughput powder diffractometer.

X-ray Structure Determination. A block-shaped single-crystal of solvated Fe-BTT (0.1 mm × 0.1 mm × 0.1 mm) was coated in Paratone-N oil, attached to a Kapton loop, and mounted on a Bruker X8 APEX diffractometer equipped with a Bruker MICROSTAR Cu rotating anode X-ray source. The sample was cooled to 100 K under a stream of nitrogen, and preliminary cell data were obtained to yield a cubic Laue group. A full hemisphere of data was collected over a period of 24 h, after which time the crystal showed no significant decomposition or structural distortion. Data were integrated and corrected for Lorentz, polarization, and absorption effects within the APEX 2 software package. Crystal and refinement parameters are listed in Table S1. Space group determinations were made based on systematic absences, *E* statistics, and successful refinement of the structure. The structure solution was obtained using direct methods and the SHELXS-97 software, and expanded through successive difference Fourier maps. Thermal parameters for all non-hydrogen atoms were refined anisotropically, and hydrogen atoms were assigned to ideal positions using the appropriate AFIX commands. Complete modeling of the solvent within the pores was not possible due to disorder, hence the electron density within the cavities was masked using the SQUEEZE routine within the PLATON software package.[2]

Accessible Surface Area Calculation. The source code for the accessible surface area calculation program was obtained free of charge from the Internet.[3] The crystallographic information file (CIF) obtained from the single crystal X-ray structure was converted to the XYZ file format using Mercury CSD 2.0. The XYZ file and UFF force field atomic parameters[4] were used as input for the simulation (atomic diameters (Å): H 2.571, C 3.431, N 3.260, O 3.118, Fe 2.594, Cl 3.516), and the accessible surface area was evaluated using a dinitrogen-sized probe molecule (diameter = 3.681 Å) inserted at randomized points in the unit cell, and averaging the resultant individual accessible surface area values after 5000 trials.

Mössbauer Spectroscopy. The Mössbauer spectrum of Fe-BTT was measured at various temperatures between 10 and 295 K in a Janis Supervaritemp cryostat with a constant-acceleration spectrometer which utilized a rhodium matrix cobalt-57 source, and was calibrated at 295 K with α-iron powder. The absorber contained 32 mg/cm^2 of powder mixed with boron

nitride. The absorber was prepared and inserted into the cryostat under dry dinitrogen. The relative statistical errors associated with the isomer shifts, quadrupole splittings, line widths, percent areas, and absolute areas measured between 10 to 225 K was ±0.005, ±0.01, ±0.01 mm/s, 0.2 %, and 0.3 (%ε)(mm/s), respectively; these statistical errors are approximately twice as large between 260 and 295 K. The absolute errors of these parameters were approximately twice the statistical errors.

Powder Neutron Diffraction Experiments. Neutron powder diffraction data were collected on the High Resolution Neutron Powder Diffractometer BT-1 at the NIST Center for Neutron Research (NCNR) with a Ge-(311) monochromator and using in-pile collimation of 15 min of arc, corresponding to a wavelength of 2.0787 Å. Measurements were taken as a function of deuterium loading at a temperature of 4 K with measurement times of ca. 9 h for the bare framework and D_2 loadings of 4.1, 8.0 D_2 molecules per formula unit, and ca. 5 h for all higher D_2 loadings.

All sample transfers were performed in a helium-filled glovebox equipped with water and oxygen monitors. Initial sample activation was performed in a glass tube with a packless bellows valve attached. The sample was evacuated using a turbomolecular pump (10^{-5} Torr) and heated to 135 °C with a ramp speed of ca. 0.5 °C per minute. After degassing at 135 °C for 16 h, the sample was cooled and transferred to a cylindrical vanadium can (i.d. 0.95 cm) equipped with a capillary gas line and a packless valve, and sealed with a lead O-ring. The sample was mounted onto a sample stick equipped with a stainless-steel gas line with an additional valve for a top-loading closed-cycle helium refrigerator. The sample was further degassed in situ for ca. 20 min under high vacuum. During the experiments, a known amount of hydrogen (deuterium) gas was loaded into the sample (813 mg), which was maintained at a temperature of 60 K until no pressure drop was observed for at least 1 min. The sample was then cooled down to the base temperature of 3.5 K over a period of 1 h in order to perform measurements. In all cases, the outgas pressure reading was zero well before reaching 25 K.

A diffraction pattern was collected for Fe-BTT prior to dosing with D_2. Subsequent Rietveld analysis indicated the existence of extra neutron density close to the Fe^{2+} ions in the framework skeleton, as expected due to the presence of residual methanol molecules. Accordingly, the extra neutron density was modeled using a partial occupancy of methanol O and C atoms, and this corrected “bare” model was used as a baseline for all subsequent

measurements involving D_2. A significant quantity of nuclear density was observed in a position approximately 4.23 Å above the chloride ion, which could be modeled as extraframework Fe atoms with the correct occupancy to fulfill charge balance of the anionic framework.

Neutron scattering diffraction patterns were analyzed using the Rietveld refinement method. The program EXPGUI incorporating the Rietveld program GSAS[5] was used to perform all refinements. The model of the bare material was refined first, and it was used as the starting point for subsequent refinements of the D_2-loaded samples. Deuterium molecules are treated as point scatters with double occupancy since they are expected to be quantum mechanically averaged in the ground state. As mentioned, during the refinement of the model for the bare material, extra C and O atoms were introduced to account for the scattering intensities from the residual methanol molecules bound to the intraframework Fe^{2+} ions. The information on the extra atoms was obtained from the diffraction pattern of the bare material and was fixed at these values when analyzing the cases with deuterium molecules loaded. The coordinates of all other atoms and the Debye-Waller factors were allowed to vary during the refinement of each deuterium loading case. Based on the structure obtained from the diffraction pattern of the bare material, the diffraction patterns of the first D_2-loaded case (4 D_2 molecules/formula unit) was analyzed by firstly neglecting the D_2 molecules. The Fourier difference maps were calculated, clearly indicating the positions of D_2 adsorption sites. Accurate values for the D_2 locations and occupancy numbers were then obtained by Rietveld refinement. For each successive D_2 loading, the Fourier difference map was calculated on the basis of the results of the previous D_2 loading and used to identify new D_2 adsorption sites.

Inelastic Neutron Scattering Experiments. Inelastic neutron scattering data were collected on the Filter Analyzer Neutron Spectrometer (FANS) BT-4 at the NCNR. The same sample can from the diffraction experiment was used and was cooled in the same manner as the neutron diffraction experiments.

Low-Pressure Gas Sorption Measurements. Glass sample tubes of a known weight were loaded with approximately 200 mg of sample, and sealed using a TranSeal. Samples were degassed at 135 °C for 24 h on a Micromeritics ASAP 2020 analyzer until the outgas rate was no more than 1 mTorr/min. The degassed sample and sample tube were weighed precisely and then transferred back to the analyzer (with the TranSeal preventing exposure of the sample to the air after degassing). The outgas rate was again confirmed to be less than 1 mTorr/min. Adsorption

isotherms were measured at 77 K in a liquid nitrogen bath for H_2 and N_2, and at 87 K in a liquid argon bath for H_2.

High-Pressure Gas Sorption Measurements. In a typical measurement, at least 200 mg of sample was loaded in a sample holder in a glove box under an argon atmosphere. The sample was evacuated at 130 °C for 10 h under a pressure of less than 10^{-5} torr. Hydrogen excess adsorption measurements were performed on an automated Sieverts' apparatus (PCTPro-2000 from Hy-Energy Scientific Instruments LLC) over a pressure range of 0-100 bar. UHP-grade hydrogen and helium (99.999% purity) were used for all measurements. Volumetric measurements at 77 K were carried out by submerging the sample holder in a liquid nitrogen bath, for which the fill-level was maintained constant throughout the experiment.

The total adsorption, C_{tot} was calculated using the following relationship;

$$C_{tot} = C_{exc} + \frac{100 \times d_g V_{pore}}{1 + d_g V_{pore}}$$

where C_{exc} is the excess uptake, d_g represents the density of pure H_2 gas calculated from an isothermal equation of state,[6] V_{pore} is the pore volume of the sample. V_{pore} is readily calculated from the experimental skeletal density of the sample, d_{sk}, and the crystallographically determined bulk density of the sample, d_{bulk}, using the expression below;

$$V_{pore} = \frac{d_{sk} - d_{bulk}}{d_{sk} d_{bulk}}$$

The total volumetric uptake, C_{vol}, was calculated by;

$$C_{vol} = Q_{ads}\, d_{bulk}$$

where Q_{ads} represents the total H_2 adsorbed (in mmol/g). Alternatively, the excess volumetric uptake can be calculated if the excess quantity of H_2 is used in place of Q_{ads}.

Other Physical Measurements. Powder X-ray diffraction patterns were obtained on a Bruker D8 Advance diffractometer with a Cu anode (λ = 1.5406 Å), or in the case of the high-throughput experiments a Bruker D8 Discover with GADDS. Infrared spectra were obtained on a Perkin-Elmer Spectrum 100 Optica FTIR spectrometer furnished with an attenuated total reflectance accessory (ATR). Carbon, hydrogen, and nitrogen analyses were obtained from the Microanalytical Laboratory at the University of California, Berkeley. Thermogravimeteric analyses (TGA) were performed on a TA Instruments TGA 5000 instrument at a ramp rate of 2 °C/min under a flow of nitrogen.

References

(1) Dincă, M.; Dailly, A.; Liu, Y.; Brown, C. M.; Neumann, D. A.; Long, J. R. *J. Am. Chem. Soc.* **2006**, *128*, 16876.

(2) Spek, A. L. *J. Appl. Crystallogr.* **2003**, *36*, 7.

(3) Accessible Surface Area Calculation Program, website address (August 2009): http://www.see.ed.ac.uk/~tduren/research/surface_area/.

(4) Rappe, A. K.; Casewit, C. J.; Colwell, K. S.; Goddard, W. A.; Skiff, W. M. *J. Am. Chem. Soc.* **1992**, *114*, 10024.

(5) Larson, A. C.; Von Dreele, R. B. *General Structure Analysis System (GSAS)*, Los Alamos National Laboratory Report LAUR 86-748 (2000).

(6) Lemmon, E. W.; McLinden, M. O.; Friend, D. G. Thermophysical Properties of Fluid Systems. In *NIST Chemistry WebBook, NIST Standard Reference Database Number 69*; Linstrom, P. J., Mallard, W. G., Eds.; National Institute of Standards and Technology, Gaithersburg MD; http://webbook.nist.gov (retrieved August 26, 2009).

Table S1. Crystallographic parameters for the crystal structure of Fe-BTT.

Crystallographic Parameter	Observed Value
Formula	$C_{12}H_4Cl_{0.5}Fe_2N_{16}O_2$
FW	533.74
T, K	100(2)
Wavelength, Å	1.54178
Crystal system, space group	Cubic, *Pm*-3*m*
Z	6
a, Å	18.8235(11)
V, Å^3	6669.6(7)
d_{calc}, g/cm^3	0.797
Absorption coefficient, mm^{-1}	5.719
F(000)	1587
Crystal size, mm^3	0.10 × 0.10 × 0.10
Theta range for data collection	2.35-65.41
Index range	$-20 \leq h \leq 20$, $-21 \leq k \leq 22$, $-14 \leq l \leq 20$
Reflections collected	22659
Independent reflections	1207
Data/restraints/parameters	1207 / 0 / 47
GOF on F^2	1.075
Largest diff. peak and hole, e·A^{-3}	0.60 and -0.26
R_1, [I>2σ(I)]	3.53
R_1(wR_2)[a], all data	3.72 (9.90)

[a]$R_1 = \Sigma||F_o|-|F_c||/ \Sigma|F_o|$, $wR_2 = \{\Sigma[w(F_o^2-F_c^2)^2]/ \Sigma[w(F_o^2)^2]\}^{1/2}$

Table S2. Mössbauer Spectral Parameters for **1-DMF**[a]

T, K	*δ*, mm/s[b]	ΔE_Q, mm/s	*Γ*, mm/s	*Area,*[c] *%*	*Area,* (%*ε*)(mm/s)	Assignment
295	0.45	0.84	0.45	4.75	6.04	$[Fe^{III}(DMF)_6]^{3+}$
	1.28	2.05	0.300(3)	4.27	-	$[Fe^{II}(DMF)_6]^{2+}$
	1.038(1)	1.772(4)	0.300(3)	90.98	-	$[(Fe^{II}_4Cl)_3(BTT)_8]^{3-}$
277	0.47	0.83	0.45	4.75	7.22	$[Fe^{III}(DMF)_6]^{3+}$
	1.28	2.15	0.37(1)	4.27	-	$[Fe^{II}(DMF)_6]^{2+}$
	1.046(3)	1.94(2)	0.37(1)	90.98	-	$[(Fe^{II}_4Cl)_3(BTT)_8]^{3-}$
260	0.49	0.82	0.45	4.75	7.78	$[Fe^{III}(DMF)_6]^{3+}$
	1.29	2.25	0.41(1)	4.27	-	$[Fe^{II}(DMF)_6]^{2+}$
	1.060(2)	2.09(3)	0.41(1)	90.98	-	$[(Fe^{II}_4Cl)_3(BTT)_8]^{3-}$
225	0.51	0.80	0.45	4.75	8.71	$[Fe^{III}(DMF)_6]^{3+}$
	1.29	2.35	0.357(5)	4.27	-	$[Fe^{II}(DMF)_6]^{2+}$
	1.077(1)	2.29(4)	0.357(5)	90.98	-	$[(Fe^{II}_4Cl)_3(BTT)_8]^{3-}$
155	0.54	0.84	0.45	4.75	10.88	$[Fe^{III}(DMF)_6]^{3+}$
	1.18	2.01	0.336(1)	4.27	-	$[Fe^{II}(DMF)_6]^{2+}$
	1.113(5)	2.560(5)	0.336(1)	90.98	-	$[(Fe^{II}_4Cl)_3(BTT)_8]^{3-}$
85	0.58	0.88	0.45(3)	4.75	12.84	$[Fe^{III}(DMF)_6]^{3+}$
	1.33	2.72	0.329(5)	4.27	-	$[Fe^{II}(DMF)_6]^{2+}$
	1.144(2)	2.774(5)	0.329(5)	90.98	-	$[(Fe^{II}_4Cl)_3(BTT)_8]^{3-}$
60	0.65	0.85	0.44(2)	4.75	13.64	$[Fe^{III}(DMF)_6]^{3+}$
	1.35	2.94	0.350(4)	4.27	-	$[Fe^{II}(DMF)_6]^{2+}$
	1.152(1)	2.812(4)	0.350(4)	90.98	-	$[(Fe^{II}_4Cl)_3(BTT)_8]^{3-}$
10	0.65	0.92	0.43(2)	4.75	14.48	$[Fe^{III}(DMF)_6]^{3+}$
	1.35	2.90	0.353(5)	4.27	-	$[Fe^{II}(DMF)_6]^{2+}$
	1.158(1)	2.857(6)	0.353(5)	90.98	-	$[(Fe^{II}_4Cl)_3(BTT)_8]^{3-}$

[a]Statistical errors are given and the absence of an error indicates that the parameter was constrained to the value given in the final refinement. The average parameters are given for the $[(Fe^{II}_4Cl)_3(BTT)_8]^{3-}$ anion. [b]The isomer shifts are given relative to 295 K *α*-iron powder. [c]The relative areas have been constrained to the values observed at 10 K and have a statistical accuracy of ±0.2 %.

Table S3. Site-specific D_2 occupancies and refinement details for the first four binding sites within Fe-BTT determined by powder neutron diffraction.

D_2 loading (molecules/f.u.)	**Site I**	**Site II**	**Site III**	**Site IV**	**Total D_2 refined**	**Rietveld fit parameter (χ^2)**
Bare framework	0	0	0	0	**0**	1.271
4.1	0.459±0.031	0.455±0.038	0	0	**4.12**	1.154
8.1	0.679±0.021	1.423±0.030	0	0	**8.40**	1.063
20.4	0.712±0.037	1.872±0.053	1.024±0.036	0.828±0.073	**21.0**	1.177
32.6	0.852±0.052	2.000±0.0	1.731±0.054	0.588±0.038	**33.3**	0.961
65.1	0.842±0.037	2.000±0.0	1.956±0.053	1.438±0.039	**63.8**	1.140
97.7	0.735±0.067	2.000±0.0	1.209±0.048	1.804±0.067	**97.6**	0.947

Table S4. Rietveld refinement for an evacuated sample of Fe-BTT (a = 18.8754(2) Å)

	x	y	z	Multiplicity	Occupancy	U_{iso}(Å^2)
Fe1	0.13538	0.5	0	12	1	0.01451
C1	0.1516	0.33575	-0.1516	24	1	0.03897
C2	0.18004	0.27115	0.18004	24	1	0.02365
C3	0.24227	0.24227	0.14984	24	1	0.02957
Cl1	0	0.5	0	3	1	0.0075
N1	0.13108	0.42056	0.08167	48	1	0.02142
N2	0.17569	0.36802	0.09165	48	1	0.02718
H1	0.26572	0.26572	0.10595	24	1	0.06904
Fe2	0.27613	0	0	6	0.25	0.04835
O2a	0.24601	0.5	0	12	0.31992	0.02327
C2a	0.3	0.5	0.03524	24	0.15996	0.02327
H2a	0.29245	0.5	0.09581	24	0.15996	0.02327
H2b	0.346	0.45522	0	12	0.31992	0.02327

*Note: Atoms O2a, C2a, H2a, and H2b constitute a methanol molecule in partial occupancy

Table S5. Rietveld refinement for an sample of Fe-BTT dosed with 4 D_2 molecules per formula unit (a = 18.8793(3) Å)

	x	y	z	Multiplicity	Occupancy	U_{iso}(Å)
Fe1	0.13504	0.5	0	12	1	0.01233
C1	0.15002	0.33481	0.15002	24	1	0.01953
C2	0.18	0.2727	-0.18	24	1	0.02541
C3	0.24175	0.24175	0.14967	24	1	0.03236
Cl1	0	0.5	0	3	1	0.00787
N1	0.13112	0.42183	0.08158	48	1	0.01504
N2	0.17533	0.36701	0.09095	48	1	0.02327
H1	0.26697	0.26697	0.10188	24	1	0.04405
Fe2	0.27613	0	0	6	0.25	0.04835
O2a	0.246	0.5	0	12	0.32	0.02136
C2a	0.299	0.5	0.03524	24	0.16	0.02136
H2a	0.29245	0.5	0.09581	24	0.6	0.02136
H2b	0.346	0.45522	0	12	0.32	0.02136
D1	0.25072	0.5	0	12	0.45894	0.17041
D2	0.32171	0	0	6	0.45484	0.37288

*Note: Atoms O2a, C2a, H2a, and H2b constitute a methanol molecule in partial occupancy

Table S6. Rietveld refinement for an sample of Fe-BTT dosed with 8 D_2 molecules per formula unit (a = 18.8815(3) Å)

	x	y	z	Multiplicity	Occupancy	U_{iso}(Å)
Fe1	0.13508	0.5	0	12	1	0.00961
C1	0.14969	0.33502	0.14969	24	1	0.02373
C2	0.18008	0.27143	0.18008	24	1	0.02991
C3	0.24153	0.24153	0.14884	24	1	0.02949
Cl1	0	0.5	0	3	1	0.02225
N1	0.1311	0.42139	0.08153	48	1	0.02188
N2	0.1753	0.36692	0.09133	48	1	0.02608
H1	0.26621	0.26621	0.10504	24	1	0.08243
Fe2	0.27613	0	0	6	0.25	0.04835
O2a	0.246	0.5	0	12	0.32	0.02136
C2a	0.2999	0.5	0.03524	24	0.16	0.02136
H2a	0.29245	0.5	0.09581	24	0.16	0.02136
H2b	0.346	0.45522	0	12	0.32	0.02136
D1	0.25332	0.5	0	12	0.6792	0.11914
D2	0.32067	0	0	6	1.42312	0.13834

*Note: Atoms O2a, C2a, H2a, and H2b constitute a methanol molecule in partial occupancy

Table S7. Rietveld refinement for an sample of Fe-BTT dosed with 20 D_2 molecules per formula unit (a = 18.8819(3) Å)

	x	y	z	Multiplicity	Occupancy	U_{iso}(Å^2)
Fe1	0.13527	0.5	0	12	1	0.01551
C1	0.15041	0.33544	-0.15041	24	1	0.01131
C2	0.18015	0.27202	-0.18015	24	1	0.03383
C3	0.24171	0.24171	-0.15161	24	1	0.02958
Cl1	0	0.5	0	3	1	0.01098
N1	0.13065	0.42222	-0.08142	48	1	0.0187
N2	0.17604	0.3678	-0.0913	48	1	0.02613
H1	0.26889	0.26889	-0.10276	24	1	0.05369
Fe2	0.27613	0	0	6	0.25	0.04835
O2a	0.246	0.5	0	12	0.32	0.02136
C2a	0.2999	0.5	0.03524	24	0.16	0.02136
H2a	0.29245	0.5	0.09581	24	0.16	0.02136
H2b	0.346	0.45522	0	12	0.32	0.02136
D1	0.25312	0.5	0	12	0.71161	0.14777
D2	0.31726	0	0	6	1.87237	0.17869
D3	0.5	0.21059	0.21059	12	1.02364	0.07549
D4	0.29682	0.29682	0	12	0.82795	0.64098

*Note: Atoms O2a, C2a, H2a, and H2b constitute a methanol molecule in partial occupancy

Table S8. Rietveld refinement for an sample of Fe-BTT dosed with 32 D_2 molecules per formula unit (a = 18.8814(4) Å)

	x	y	z	Multiplicity	Occupancy	U_{iso}(Å^2)
Fe1	0.13532	0.5	0	12	1	0.00951
C1	0.14988	0.33541	-0.14988	24	1	0.02362
C2	0.18232	0.27437	-0.18232	24	1	0.04545
C3	0.2421	0.2421	-0.1508	24	1	0.03559
Cl1	0	0.5	0	3	1	0.01433
N1	0.13046	0.42125	-0.08253	48	1	0.02015
N2	0.17663	0.3678	-0.09064	48	1	0.02422
H1	0.26887	0.26887	-0.10316	24	1	0.03721
Fe2	0.27613	0	0	6	0.25	0.04835
O2a	0.246	0.5	0	12	0.32	0.02136
C2a	0.2999	0.5	0.03524	24	0.16	0.02136
H2a	0.29245	0.5	0.03524	24	0.16	0.02136
H2b	0.346	0.15522	0	12	0.32	0.02136
D1	0.25293	0.5	0	12	0.85207	0.18113
D2	0.32394	0	0	6	2	0.18192
D3	0.5	0.21224	0.21224	12	1.73127	0.13953
D4	0.33396	0.33396	0	12	0.58758	0.05891
D5	0.20693	0.15153	0	24	0.68973	0.27221

*Note: Atoms O2a, C2a, H2a, and H2b constitute a methanol molecule in partial occupancy

Table S9. Rietveld refinement for an sample of Fe-BTT dosed with 65 D_2 molecules per formula unit (a = 18.8830(3) Å)

	x	y	z	Multiplicity	Occupancy	U_{iso}(Å^2)
Fe1	0.1362	0.5	0	12	1	0.008
C1	0.15087	0.33755	-0.15087	24	1	0.01248
C2	0.18224	0.27487	-0.18224	24	1	0.01784
C3	0.24145	0.24145	-0.15089	24	1	0.03387
Cl1	0	0.5	0	3	1	0.02041
N1	0.13138	0.42161	-0.08224	48	1	0.01584
N2	0.1765	0.36878	-0.09145	48	1	0.02095
H1	0.26775	0.26775	-0.10528	24	1	0.05029
Fe2	0.27613	0	0	6	0.25	0.5087
O2a	0.246	0.5	0	12	0.32	0.12677
C2a	0.2999	0.5	0.03524	24	0.16	0.12677
H2a	0.29245	0.5	0.03524	24	0.16	0.12677
H2b	0.346	0.15522	0	12	0.32	0.12677
D1	0.25196	0.5	0	12	0.84242	0.07274
D2	0.31808	0	0	6	2	0.27553
D3	0.5	0.21127	0.21134	12	1.9561	0.13768
D4	0.32973	0.32973	0	12	1.43781	0.11457
D5	0.21243	0.14869	0	24	1.1303	0.18157
D6	0.31181	0.31181	0.31181	8	1.37178	0.18077
D7	0.36543	0.36543	0.13605	24	0.9225	0.28724
D8	0.10764	0.10764	0.10764	8	0.56105	0.26638

*Note: Atoms O2a, C2a, H2a, and H2b constitute a methanol molecule in partial occupancy

Table S10. Rietveld refinement for an sample of Fe-BTT dosed with 98 D_2 molecules per formula unit (a = 18.8897(6) Å)

	x	y	z	Multiplicity	Occupancy	U_{iso}(Å^2)
Fe1	0.1357	0.5	0	12	1	-0.00879
C1	0.15156	0.33934	-0.15156	24	1	0.00598
C2	0.1832	0.27505	-0.1832	24	1	0.02736
C3	0.24108	0.24108	-0.15032	24	1	0.03072
Cl1	0	0.5	0	3	1	0.01667
N1	0.13219	0.41996	-0.08292	48	1	0.01459
N2	0.17783	0.36991	-0.09368	48	1	0.0139
H1	0.2704	0.2704	-0.10691	24	1	0.0105
Fe2	0.27613	0	0	6	0.25	0.04835
O2a	0.246	0.5	0	12	0.32	0.02136
C2a	0.2999	0.5	0.03524	24	0.16	0.02136
H2a	0.29245	0.5	0.03524	24	0.16	0.02136
H2b	0.346	0.15522	0	12	0.32	0.02136
D1	0.2578	0.5	0	12	0.73433	0.10553
D2	0.33028	0	0	6	2	0.30127
D3	0.5	0.21343	0.21024	12	1.20863	0.17092
D4	0.32485	0.32485	0	12	1.80261	0.09872
D5	0.22757	0.13636	0	24	1.56905	0.2055
D6	0.31386	0.31386	0.31386	8	2	0.2188
D7	0.36511	0.36511	0.15366	24	1.60823	0.35825
D8	0.11259	0.11259	0.11259	8	2	0.17907
D9	0.5	0.5	0.07624	6	2	0.76756
D10	0.5	0.5	0.28114	6	0.56862	0.27481

*Note: Atoms O2a, C2a, H2a, and H2b constitute a methanol molecule in partial occupancy

Table S11. N_2 adsorption isotherm for an activated sample of Fe-BTT at 77 K.

P **(P/P_0)**	**N_2 adsorbed (cm^3/g)**
0.000001446	10.19558
0.000001295	20.39341
0.000001812	30.58989
0.000002885	40.78346
0.000004267	50.97322
0.000005952	61.15827
0.000007811	71.33818
0.00000978	81.5136
0.000011782	91.68298
0.000013774	101.8481
0.000015819	112.0081
0.000018124	122.1611
0.00002061	132.309
0.000023517	142.4483
0.000027062	152.5785
0.000031406	162.6959
0.000036612	172.8003
0.000042619	182.8893
0.000050098	192.9581
0.000058788	203.0043
0.000069548	213.0213
0.00008269	223.0041
0.000098564	232.9454
0.000118009	242.8344
0.000141535	252.661
0.00017013	262.4108
0.000204489	272.0686
0.000245669	281.6175
0.000294645	291.0349
0.000353093	300.2957
0.000422897	309.3684
0.000507764	318.2097
0.000608891	326.7519
0.000730964	334.9801
0.000877834	342.7959
0.001165195	352.7518
0.00154614	362.6202
0.00205262	372.359
0.002699745	381.9496
0.003442552	391.5404
0.004291785	400.9902
0.005254508	410.3758
0.006330633	419.5827
0.007801824	428.958
0.010092481	439.0026
0.012796943	446.6482
0.016448309	453.4094
0.021724616	460.044
0.027742761	464.9333
0.03441658	468.9406
0.04160808	472.3372
0.049202947	475.1152

Table S11 (continued)

P (P/P_0)	N_2 adsorbed (cm^3/g)
0.058194011	477.794
0.067422589	480.0188
0.076880262	481.9938
0.086023067	483.6328
0.095114156	485.0554
0.105125296	486.4406
0.186115677	493.0244
0.282812298	497.1929
0.384204925	499.8336
0.455866907	501.2105
0.545267753	502.5214
0.634050708	503.468
0.722974192	504.353
0.811666546	505.258
0.900251682	506.585

Table S12. H_2 adsorption and desorption data in an activated sample of Fe-BTT at low pressure.

T = 77 K		T = 87 K	
P **(Torr)**	**H_2 adsorbed (wt %)**	***P*** **(Torr)**	**H_2 adsorbed (wt %)**
0.00295	0.008828	0.01494	0.008716
0.00894	0.035358	0.01701	0.009989
0.0152	0.052885	0.02262	0.013655
0.02749	0.075801	0.02933	0.017806
0.05313	0.099726	0.0333	0.02011
0.09487	0.118668	0.04183	0.024755
0.13504	0.129489	0.0532	0.030263
0.17195	0.136923	0.09889	0.046935
0.27243	0.152015	0.14042	0.057584
0.33401	0.15941	0.18938	0.067147
0.68114	0.191801	0.23904	0.07481
1.10029	0.221739	0.31205	0.083738
1.50959	0.246068	0.71408	0.112508
1.81444	0.262016	1.09024	0.128349
2.11186	0.276198	1.37814	0.137832
2.38966	0.288458	1.81129	0.149859
2.92555	0.309843	2.0955	0.156839
3.95652	0.344728	2.38932	0.163517
9.00305	0.454532	3.11177	0.178597
14.5524	0.530776	3.89975	0.193099
22.07591	0.608635	8.90616	0.262801
25.27345	0.636975	12.73556	0.302595
39.70182	0.746963	19.51694	0.358525
50.07998	0.815507	30.28111	0.425851
69.4456	0.926785	37.79329	0.464137
99.93439	1.075218	52.07027	0.525379
149.3442	1.27073	71.30955	0.593555
200.1667	1.433295	100.5332	0.679943
253.9768	1.575959	153.161	0.808725
305.6611	1.692557	201.4605	0.909475
357.4756	1.794149	251.0142	1.001237
401.3574	1.871006	304.2697	1.089865
450.0386	1.947608	352.0254	1.162611
499.7745	2.018424	401.421	1.232237
551.5566	2.0856	452.0654	1.298
599.7122	2.143083	499.9107	1.356047
650.6822	2.19941	551.4488	1.41479

(Table S12, continued)

T = 77 K		T = 87 K	
P **(Torr)**	**H_2 adsorbed (wt %)**	***P*** **(Torr)**	**H_2 adsorbed (wt %)**
701.0056	2.251134	600.6662	1.467351
749.9803	2.297801	652.87	1.520353
800.2315	2.343229	700.0425	1.565403
839.5252	2.377411	750.1134	1.610869
885.4049	2.41552	800.2014	1.653677
747.7538	2.298739	842.9772	1.689818
647.9335	2.19998	889.0294	1.727002
549.2241	2.085804	750.2894	1.614012
500.0032	2.021533	697.3209	1.566582
452.2024	1.953224	597.5927	1.468303
401.2779	1.872625	549.5538	1.41703
349.9391	1.781484	501.4601	1.362272
300.2047	1.681317	452.6935	1.303107
253.9263	1.575183	401.3951	1.236311
201.6061	1.435625	352.6206	1.167212
154.7704	1.286492	300.6978	1.087258
113.8582	1.13043	254.1457	1.00915
48.87784	0.799776	203.6609	0.915201
10.17776	0.462725	153.6637	0.810337
1.19873	0.218296	107.0589	0.69607
		54.01701	0.529437
		10.42377	0.273748
		1.16491	0.124271

Table S13. Higher-pressure H_2 adsorption and desorption data in activated Fe-BTT at 77 K.

	Adsorption			Desorption	
P (bar)	Excess Uptake (wt %)	Total Uptake (wt %)	P (bar)	Excess Uptake (wt %)	Total Uptake (wt %)
0.593	2.08486	2.10722	92.673	2.14493	4.28988
1.611	2.81774	2.86357	87.434	2.24297	4.26667
2.724	3.13358	3.20504	82.207	2.35387	4.25663
3.884	3.37494	3.47309	77.030	2.46230	4.24531
5.332	3.49222	3.62369	71.721	2.57139	4.23155
6.788	3.55515	3.72009	66.691	2.69405	4.23787
8.238	3.63294	3.83119	61.659	2.80114	4.22864
9.941	3.65360	3.89095	56.626	2.91612	4.22731
11.593	3.66947	3.9447	51.613	3.01010	4.20553
13.264	3.67044	3.98397	46.732	3.10670	4.18948
14.918	3.65126	4.00268	41.727	3.18090	4.14826
16.592	3.63622	4.02596	36.693	3.26044	4.11182
18.288	3.60588	4.03439	31.740	3.34907	4.08642
19.964	3.57603	4.04285	26.770	3.46021	4.08321
21.631	3.54821	4.0531	21.583	3.55340	4.05719
23.291	3.52264	4.0654	16.608	3.63203	4.02154
24.805	3.49051	4.06777	12.350	3.66555	3.95730
26.665	3.45490	4.07453	9.173	3.63386	3.85269
28.517	3.40244	4.06425	6.814	3.56636	3.73107
30.394	3.37428	4.07877	5.042	3.47324	3.59731
32.128	3.34787	4.09175	3.773	3.32223	3.41721
34.446	3.31008	4.1066	2.829	3.13772	3.21104
36.764	3.25859	4.10767	2.125	2.97308	3.03029
39.056	3.20545	4.10647	1.618	2.82837	2.87397
41.327	3.17870	4.1311	1.245	2.64708	2.68412
43.587	3.14389	4.1474	0.963	2.46379	2.49438
45.845	3.10791	4.16239	0.757	2.30176	2.32763
48.083	3.06860	4.17359	0.599	2.13598	2.15825
49.933	3.02081	4.16749	0.481	1.98739	2.00696
52.648	2.96465	4.17247	0.386	1.84556	1.86295
55.397	2.92746	4.1971	0.317	1.73065	1.74646
58.115	2.87587	4.20657			
60.824	2.82063	4.21208			
63.513	2.75034	4.20206			
66.227	2.69532	4.20777			
68.922	2.63486	4.20753			
71.640	2.56341	4.19677			
74.355	2.50634	4.20023			
77.065	2.45351	4.20776			

(Table S13, continued)

	Adsorption	
P (bar)	**Excess Uptake (wt %)**	**Total Uptake (wt %)**
83.237	2.32387	4.21528
86.742	2.26357	4.2327
90.262	2.16966	4.21672
93.824	2.10574	4.23153

Table S14. Higher-pressure H_2 adsorption data in an activated sample of Fe-BTT at 298 K.

P (bar)	Excess Uptake (wt %)	Total Uptake (wt %)
2.0898	0.00402	0.02303
4.14545	0.00926	0.03942
6.21559	0.011	0.0524
8.28062	0.01691	0.0695
10.33081	0.02005	0.08376
12.38241	0.02828	0.10311
14.41603	0.03667	0.12252
18.52603	0.05329	0.1614
22.6187	0.07384	0.20412
26.67186	0.09485	0.24707
30.6985	0.11817	0.29217
34.65479	0.13893	0.33434
38.56031	0.16605	0.38257
42.40003	0.19384	0.43111
46.20879	0.21635	0.47419
50.01153	0.23115	0.50952
53.80813	0.26123	0.5601
57.55266	0.28027	0.59933
61.2852	0.2997	0.63889
64.98153	0.31798	0.67709
68.66608	0.33307	0.71204
72.33283	0.35577	0.75449
75.96991	0.37731	0.79561
79.55683	0.40122	0.83882
83.12951	0.42069	0.87751
86.67039	0.43467	0.91054
90.19142	0.46061	0.9554
93.71891	0.48057	0.99432
97.25838	0.50789	1.04066

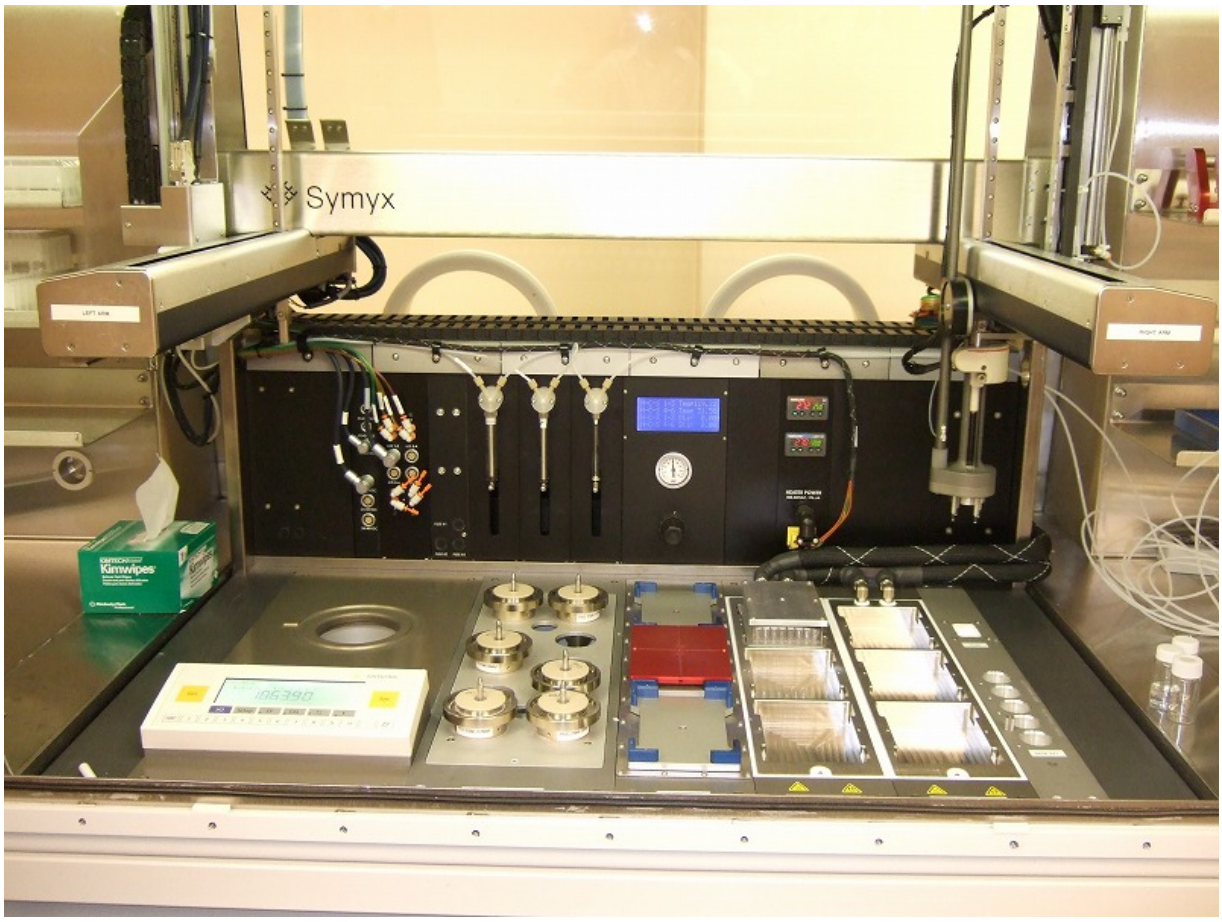

Figure S1. A view of the Symyx Core Module robot deck. The left arm consists of a gripper for holding the powder dispensing heads (circular containers in the center), and the right arm is equipped with a gripper for transferring the vials from one of the six plate positions on the right of the deck, to the balance (circular opening at the left). Liquid dispensing occurs through movements of the right arm, and the aspiration of solvents occurs through the three syringe pumps at the back of the deck.

Figure S2. A view of the custom-designed 96-vial plate loaded with 1 mL vials. The plates are placed in one of the six plate positions on the robot deck shown in Figure S1, and can be heated, cooled, or stirred according to the parameters within the experiment protocol.

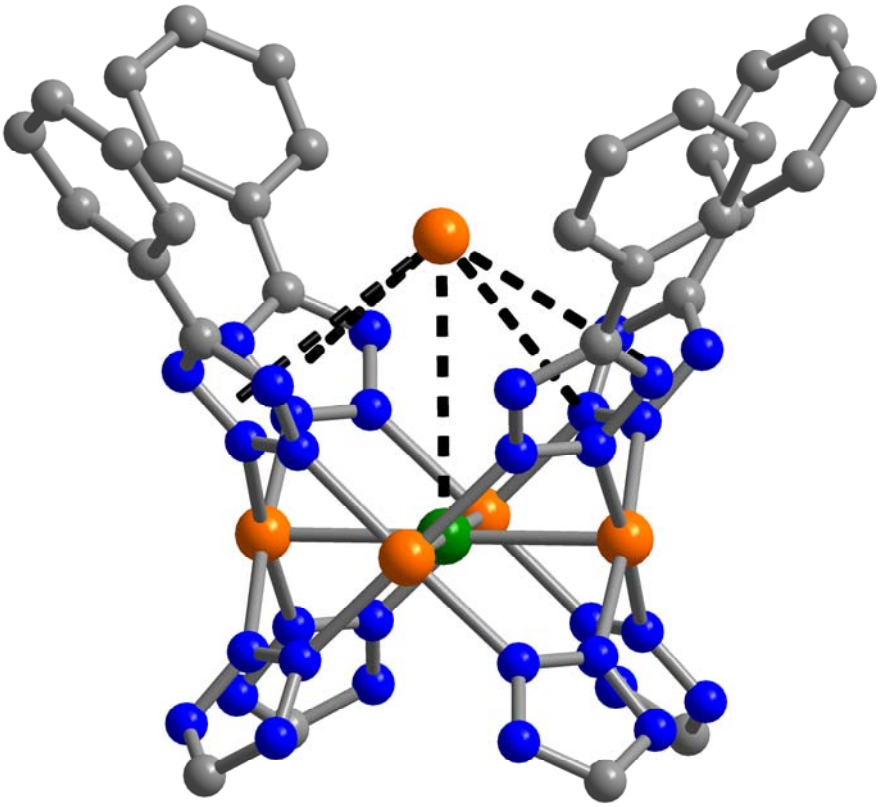

Figure S3. The location of the extraframework ions within Fe-BTT as determined by neutron diffraction. Orange, green, blue, and gray spheres represent Fe, Cl, N, and C atoms, respectively. Hydrogen atoms have been omitted for clarity. The occupancy of the extraframework ions is approximately 1/8.

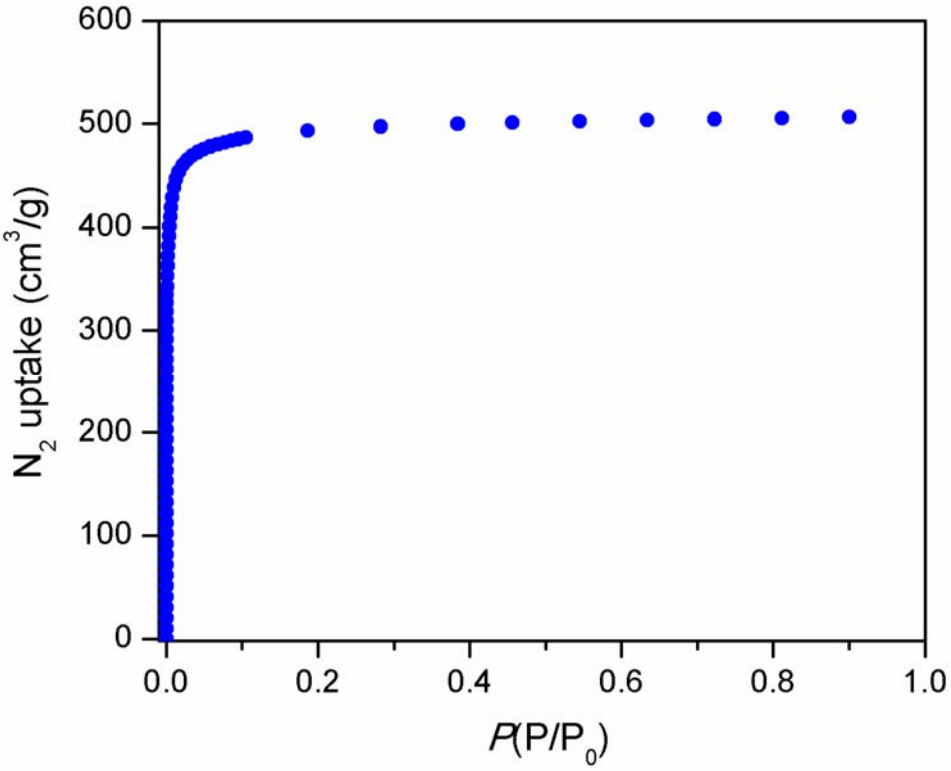

Figure S4. Adsorption isotherm for N_2 in an activated sample of Fe-BTT recorded at 77 K.

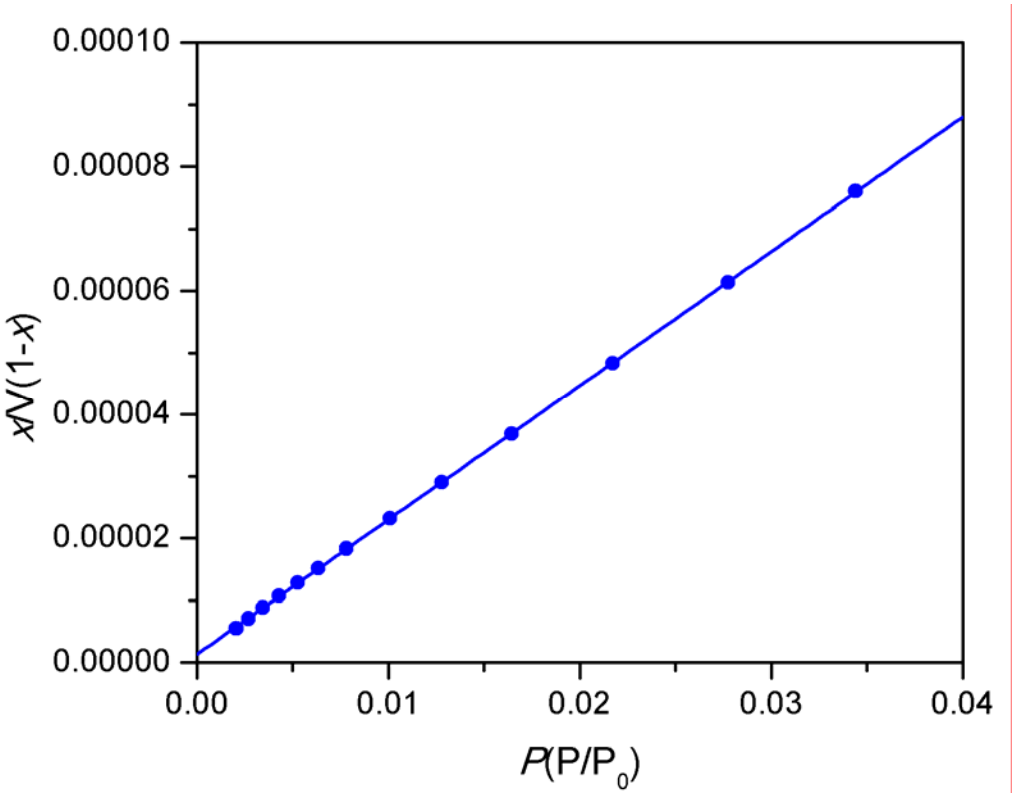

Figure S5. A BET plot of the adsorption isotherm for N_2 in Fe-BTT at 77 K, where x represents the quantity (P/P_0) and V is the volume of N_2 adsorbed. The blue line represents a linear best fit of the data points. Inset: parameters for the linear best fit and resulting constants for calculation of the BET surface area.

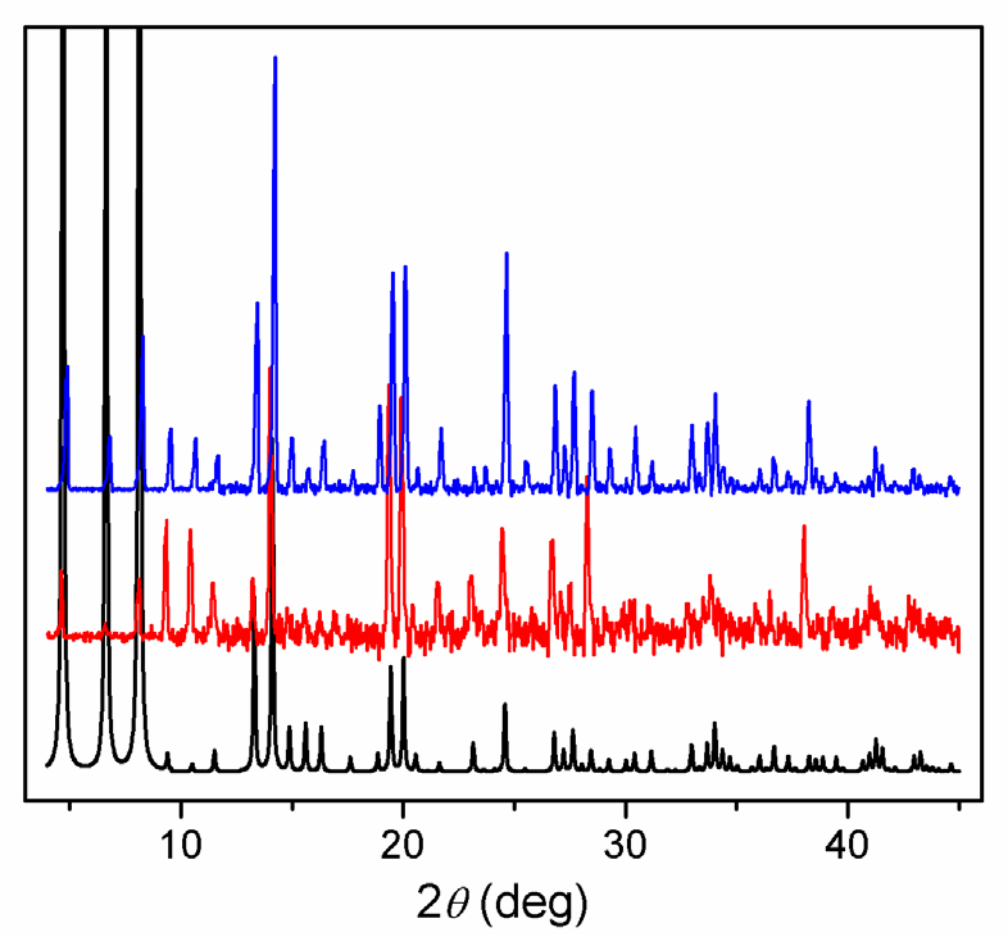

Figure S6. Powder X-ray diffraction patterns of Fe-BTT: simulated from the single crystal X-ray structure (black), of the as-synthesized solvated material (red), and the methanol-exchanged material (blue).

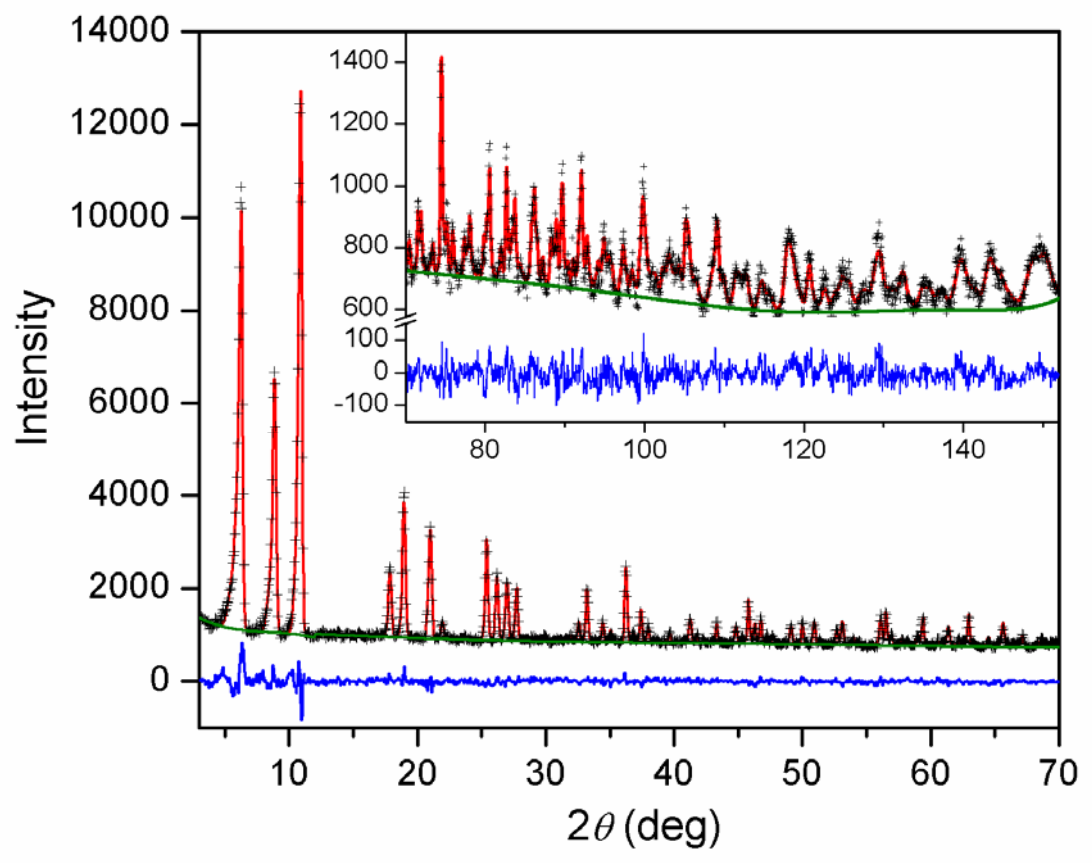

Figure S7. Rietveld refinement of neutron powder diffraction data for an evacuated sample of Fe-BTT. Green lines, crosses, and red lines represent the background, experimental, and calculated diffraction patterns, respectively. The blue line represents the difference between experimental and calculated patterns. The final Rietveld fit parameter was $\chi^2 = 1.271$.

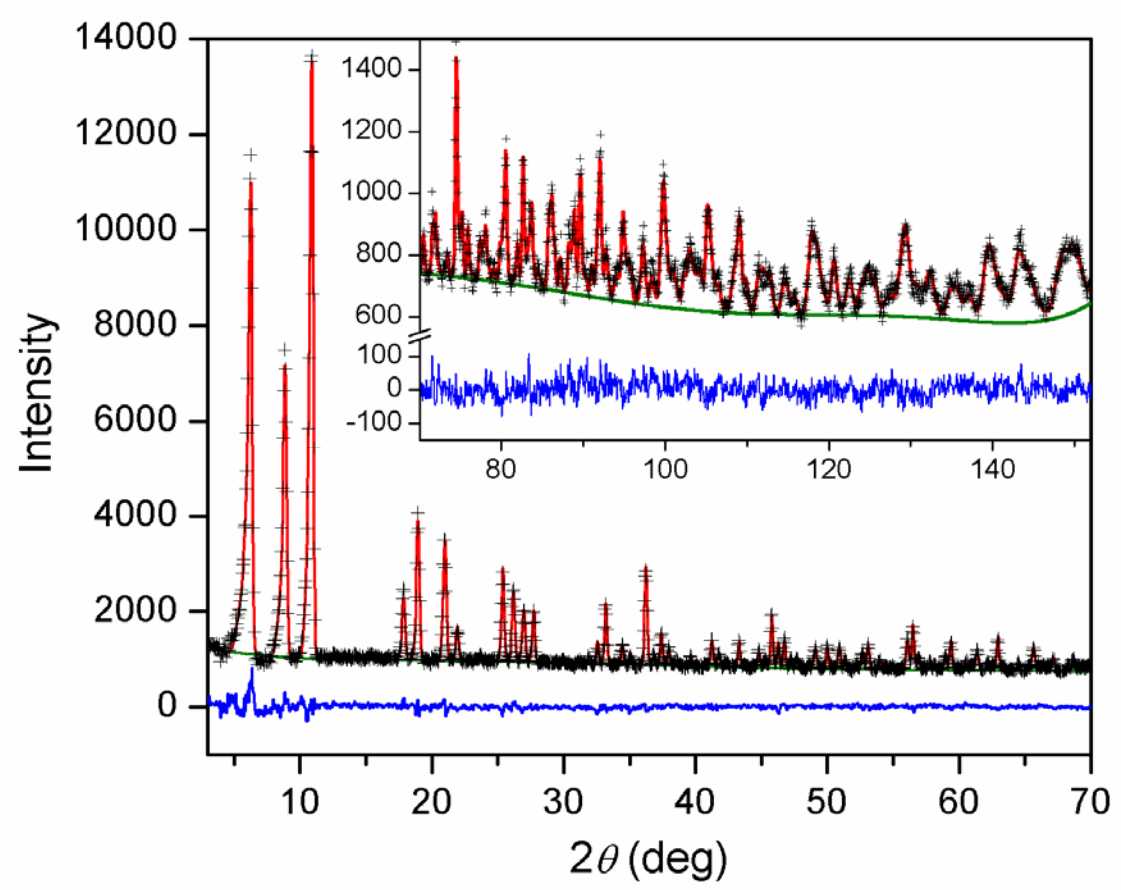

Figure S8. Rietveld refinement of neutron powder diffraction data for loading of 4 D_2 molecules per formula unit of Fe-BTT. Green lines, crosses, and red lines represent the background, experimental, and calculated diffraction patterns, respectively. The blue line represents the difference between experimental and calculated patterns. The final Rietveld fit parameter was $\chi^2 = 1.154$.

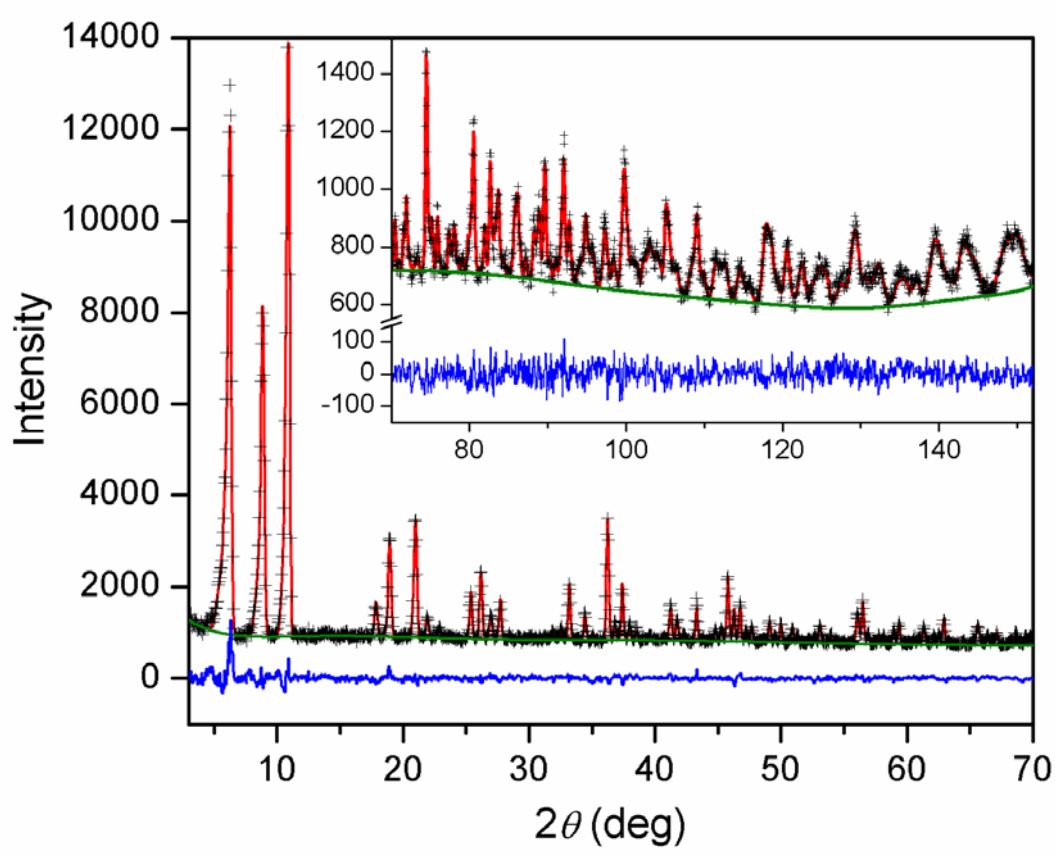

Figure S9. Rietveld refinement of neutron powder diffraction data for loading of 20 D_2 molecules per formula unit of Fe-BTT. Green lines, crosses, and red lines represent the background, experimental, and calculated diffraction patterns, respectively. The blue line represents the difference between experimental and calculated patterns. The final Rietveld fit parameter was $\chi^2 = 1.177$.

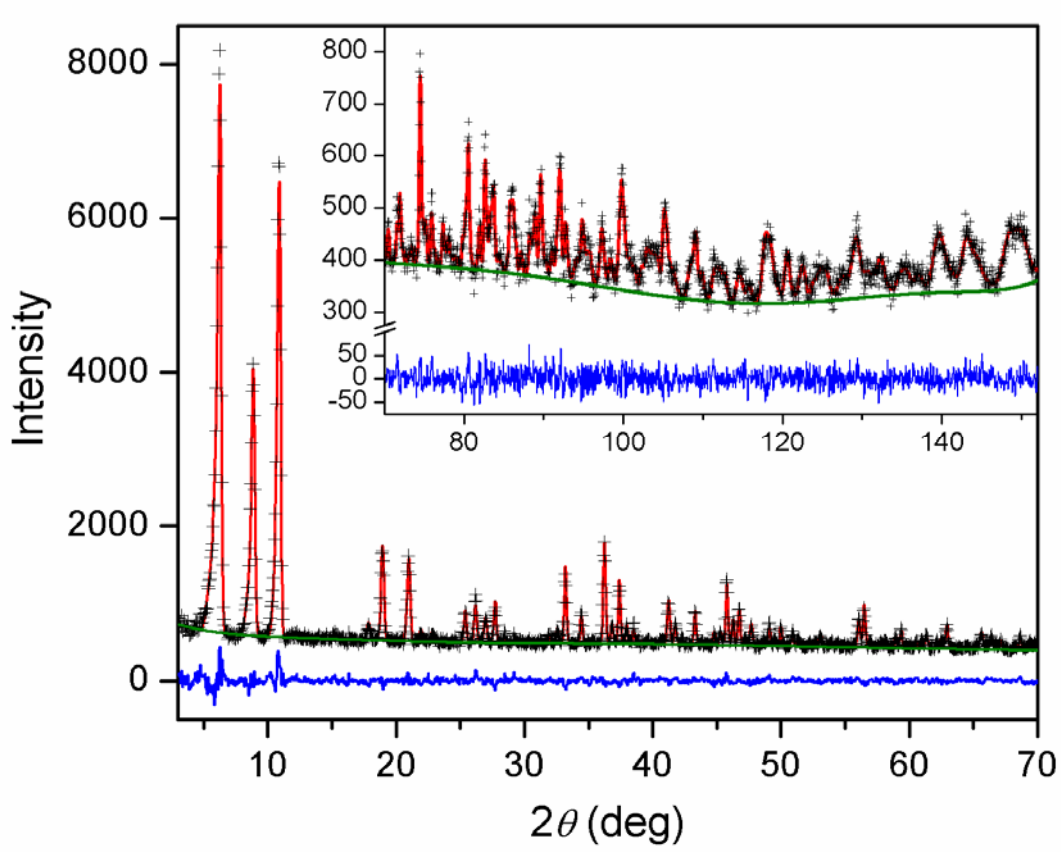

Figure S10. Rietveld refinement of neutron powder diffraction data for loading of 33 D_2 molecules per formula unit of Fe-BTT. Green lines, crosses, and red lines represent the background, experimental, and calculated diffraction patterns, respectively. The blue line represents the difference between experimental and calculated patterns. The final Rietveld fit parameter was $\chi^2 = 0.9606$.

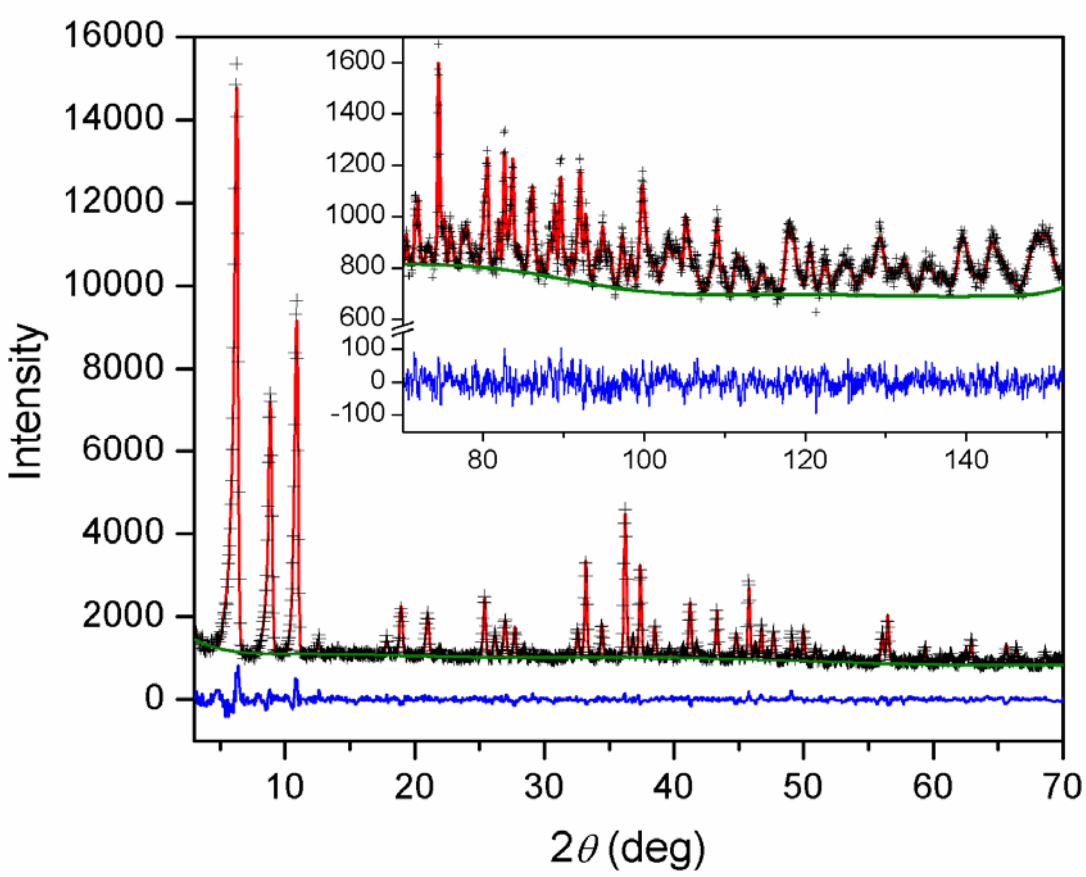

Figure S11. Rietveld refinement of neutron powder diffraction data for loading of 65 D_2 molecules per formula unit of Fe-BTT. Green lines, crosses, and red lines represent the background, experimental, and calculated diffraction patterns, respectively. The blue line represents the difference between experimental and calculated patterns. The final Rietveld fit parameter was $\chi^2 = 1.140$.

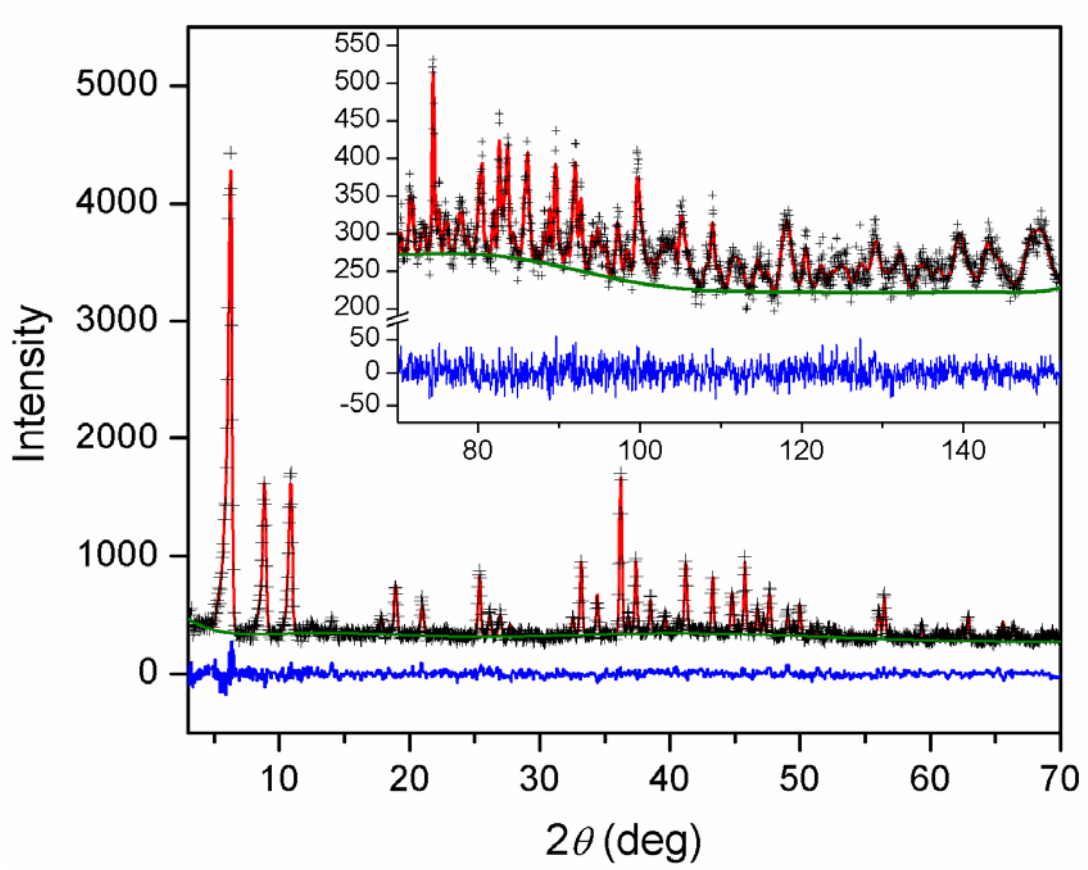

Figure S12. Rietveld refinement of neutron powder diffraction data for loading of 98 D_2 molecules per formula unit of Fe-BTT. Green lines, crosses, and red lines represent the background, experimental, and calculated diffraction patterns, respectively. The blue line represents the difference between experimental and calculated patterns. The final Rietveld fit parameter was $\chi^2 = 0.9473$.

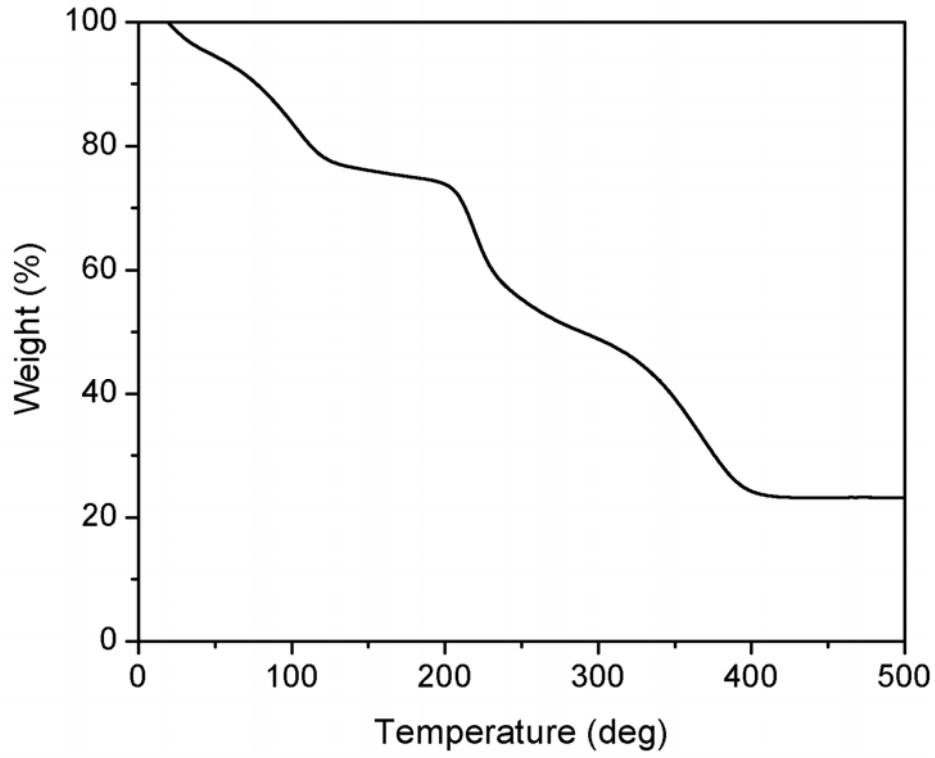

Figure S13. Thermogravimetric analysis of as-synthesized Fe-BTT up to a temperature of 500 °C, as measured using a ramping rate of 2 °C/min.

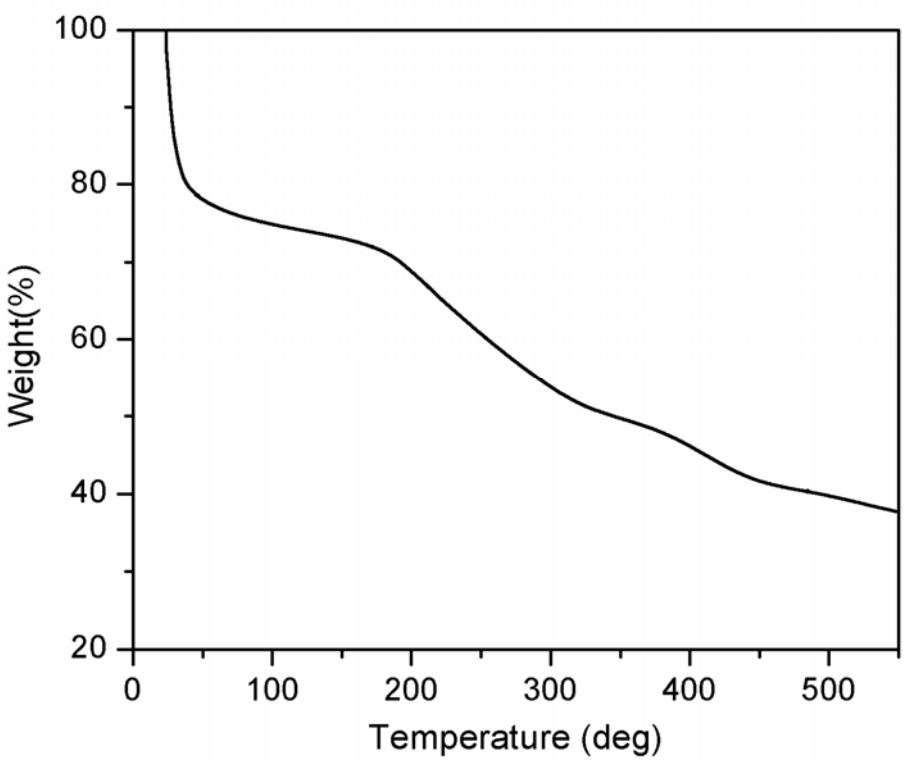

Figure S14. Thermogravimetric analysis of methanol-exchanged Fe-BTT up to a temperature of 550 °C, as measured using a ramping rate of 2 °C/min.

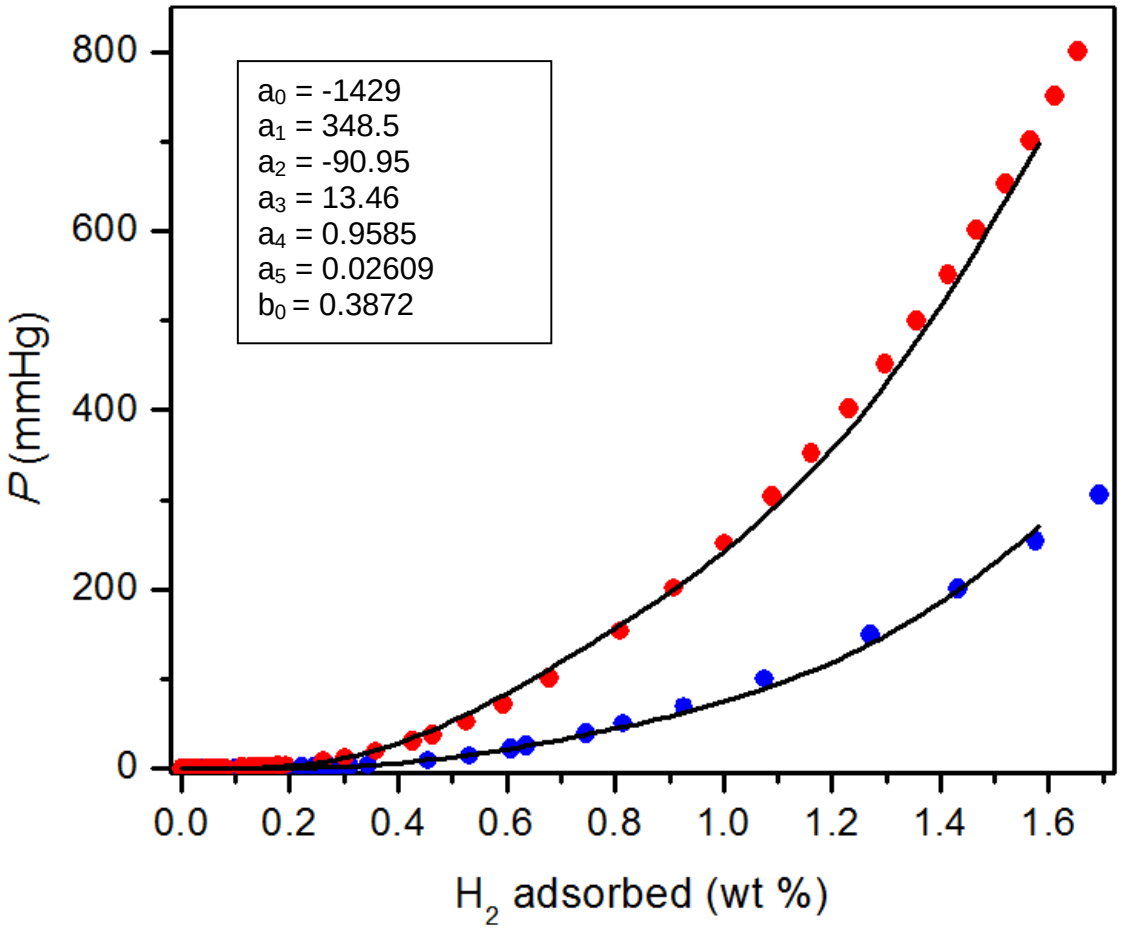

Figure S15. Fitting of the hydrogen adsorption data recorded at 77 K (blue) and 87 K (red) using a virial type function. Inset: virial parameters used for the fitting to the data.